Insights into the Molecular Relationships between Malate and Lactate Dehydrogenases: Structural and Biochemical Properties of Monomeric and Dimeric Intermediates of a Mutant of Tetrameric L-[LDH-like] Malate Dehydrogenase from the Halophilic Archaeon *Haloarcula marismortui*

Dominique Madern,*,‡ Christine Ebel,‡ Moshe Mevarech,§ Stéphane B. Richard,‡,|| Claude Pfister,‡,⊥ and Giuseppe Zaccai‡,@

Institut de Biologie Structurale, CEA-CNRS, 41 Avenue des Martyrs, F-38027 Grenoble Cedex 1, France, Department of Molecular Microbiology and Biotechnology, Tel Aviv University, Tel Aviv 69978, Israel, Université Joseph Fourier, 38000 Grenoble, France, and Institut Laue Langevin, BP 156X, 38042 Grenoble, France

Received May 3, 1999; Revised Manuscript Received October 22, 1999

ABSTRACT: L-Malate (MalDH) and L-lactate (LDH) dehydrogenases belong to the same family of NAD-dependent enzymes. LDHs are tetramers, whereas MalDHs can be either dimeric or tetrameric. To gain insight into molecular relationships between LDHs and MalDHs, we studied folding intermediates of a mutant of the LDH-like MalDH (a protein with LDH-like structure and MalDH enzymatic activity) from the halophilic archaeon *Haloarcula marismortui* (*Hm* MalDH). Crystallographic analysis of *Hm* MalDH had shown a tetramer made up of two dimers interacting mainly via complex salt bridge clusters. In the R207S/R292S *Hm* MalDH mutant, these salt bridges are disrupted. Its structural parameters, determined by neutron scattering and analytical centrifugation under different conditions, showed the protein to be a tetramer in 4 M NaCl. At lower salt concentrations, stable oligomeric intermediates could be trapped at a given pH, temperature, or NaCl solvent concentration. The spectroscopic properties and enzymatic behavior of monomeric, dimeric, and tetrameric species were thus characterized. The properties of the dimeric intermediate were compared to those of dimeric intermediates of LDH and dimeric MalDHs. A detailed analysis of the putative dimer−dimer contact regions in these enzymes provided an explanation of why some can form tetramers and others cannot. The study presented here makes *Hm* MalDH the best characterized example so far of an LDH-like MalDH.

The native state of an oligomeric protein is reached by following a pathway of various events, which prevent or favor molecular association. Small-angle neutron scattering (SANS)[1] and analytical ultracentrifugation (AUC) are powerful methods for characterizing macromolecular assembly in solution. Their combination with the biochemical characterization of the different species that are involved can yield information of important biological relevance. By using such complementary approaches, we probed the molecular properties of structural intermediates of a mutant of the LDH-like malate dehydrogenase from the halophilic archaeon *Haloarcula marismortui* (*Hm* MalDH) to provide insights into the molecular relationships between the L-malate and L-lactate dehydrogenases (MalDH and LDH, respectively).

MalDH and LDH are members of a homologous class of 2-ketoacid NAD-dependent dehydrogenases, which catalyze the conversion of 2-hydroxyacids to the corresponding 2-ketoacids (*1*, *2*). MalDH and LDH from a wide variety of organisms have been purified and characterized (*3*−*10*). They have similar three-dimensional structures and are somewhat identical in sequence, but MalDH is specific for oxaloacetate and LDH for pyruvate substrate. The important residues for substrate binding and catalysis have been identified, and active site residues in both sets of enzymes have been the target of site-directed mutagenesis that allowed modulation of substrate recognition specificity (*11*−*13*). From crystallographic studies of LDH and MalDH complexes with substrate analogues and cofactors, it has been suggested that discrimination between the two substrates was the result of a charge imbalance inside the catalytic cavity (*14*, *15*).

Full enzymatic activity in LDHs is associated with the tetrameric state of the enzyme, and dimeric intermediates are inactive or weakly active (*16*, *17*). The allosteric effector fructose 1,6-bisphosphate modulates the activity of some bacterial LDHs (*18*, *19*), whereas in the enzymes from vertebrates, activity is not allosterically regulated (*20*). The

* To whom correspondence should be addressed: Institut de Biologie Structurale, 41 Rue Jules horowitz, 38027 Grenoble Cedex 1, France. Telephone: (33) (0) 4 76 88 95 71. Fax: (33) (0) 4 76 88 54 94. E-mail: madern@ibs.fr.

‡ CEA-CNRS.

§ Tel Aviv University.

|| Present address: Structural Biology Laboratory, The Salk Institute for Biological Studies, P.O. Box 85800, San Diego, CA 92186-5800.

⊥ Université Joseph Fourier.

@ Institut Laue Langevin.

[1] Abbreviations: MalDH, L-malate dehydrogenase (EC 1.1.1.37); LDH, L-lactate dehydrogenase (EC 1.1.1.27); ANS, 1-anilinonaphthalene-8-sulfonate; AUC, analytical ultracentrifugation; CD, circular dichroism; SANS, small-angle neutron scattering; monA, monomer A; monB, monomer B; monC, monomer C; monD, monomer D; *Hm*, *Haloarcula marismortui*.

10.1021/bi9910023 CCC: $19.00
Published on Web 01/14/2000

crystallographic structures of various LDHs have been obtained, which allowed us to suggest mechanisms by which the enzymatically active tetrameric state is achieved. For example, in LDHs from *Bacillus stearothermophilus* and *Bifidobacterium longum*, the allosteric effector binds at a specific anionic site and promotes the condensation of two weakly active dimers into a fully active tetramer, with high affinity for the substrate (*21*, *22*). On the other hand, in LDH from *Thermotoga maritima*, the effect on activity of fructose 1,6-bisphosphate is not related to the oligomeric state of the enzyme (*19*). In the case of mammalian LDHs, the assembly of the tetramer depends on a long N-terminal extension (*23*). In contrast to LDH, both dimeric and tetrameric oligomeric states of MalDH were characterized as fully active enzymes without allosteric regulation (*24*, *25*).

The primary structure analysis of MalDHs showed that they have diverged into various groups. One of these displays stronger similarities with LDH than with other MalDH, suggesting the existence of a distinct so-called LDH-like MalDH group (*13*, *26*−*29*). The link between LDH and the LDH-like group of MalDHs was reinforced by the crystallographic study of *Hm* MalDH (*30*, *31*) that showed a three-dimensional structure that was similar to LDH rather than to dimeric MalDH (*32*−*35*).

Mutagenesis of protein interfaces has been a powerful approach to understanding the properties of subassemblies and their role in a complex structure (*36*, *37*). The wild type halophilic enzyme is a well-studied homotetramer (132 kDa, 303 amino acid residues per subunit), which is deactivated rapidly when the NaCl or KCl concentration of the solution is lowered below 2 M (*38*, *39*). Deactivation is concomitant with the dissociation of the tetramer into inactive unfolded monomers, with no observable intermediates (*40*). Two complex salt bridges are observed at the dimer−dimer interface of the tetramer (see Figure 4 in ref *31*). They involve Arg 207 and Arg 292 in intra- and intersubunit interactions with Glu 188, Asp 209, Asp 211, and Glu 301 (*30*, *31*). It is reasonable to assume that the intramolecular salt bridges are formed during subunit folding, and once the native state of separate molecules is reached, the intermolecular salt bridges participate in the quaternary assembly of the structure. In fact, at 3.2 Å resolution, they appeared to be the only interdimer interactions stabilizing the tetramer. It was expected, therefore, that their disruption would lead to the dissociation of the tetramer into dimers A−B and D−C (according to the nomenclature in ref *31*). To test this hypothesis, Arg 207 and Arg 292, both involved in the complex salt bridges, were mutated to serines, as serines at these equivalent positions were most frequently found in other MalDHs (sequence alignment not shown).

This report describes the results of a set of complementary biophysical methods, which showed that the R207S/R292S *Hm* MalDH mutant can be found in different oligomeric states depending on the pH and salt and protein concentration. A comparative structural analysis of the *Hm* MalDH, now determined to 2.6 Å resolution (*31*), with dimeric MalDH and LDH elucidated the mechanism by which the tetrameric state is obtained. From these results, it was possible to draw a folding−unfolding pathway that establishes a new link between MalDH and LDH molecular groups.

MATERIALS AND METHODS

NADH and oxaloacetate were from Sigma. Chromatographic resins were from Whatman (DEAE-cellulose DE52) or Pharmacia (Sepharose 4B, Superose 12HR, and hydroxyapatite). All other chemicals were from Merck.

Site-Directed Mutagenesis. The gene encoding the halophilic MalDH was cloned into M13mp18 phage, and site-directed mutagenesis was performed using the Oligonucleotide Directed in Vitro Mutagenesis System, version 2 (Amersham). The system of numbering residues is taken from ref *31*.

Protein Preparation. Expression, renaturation, and purification of recombinant *Hm* MalDH have been described previously (*13*, *41*).

Enzymatic Assay. (1) Standard Assay. The enzyme solution was mixed with 1 mL of 4 M NaCl and 50 mM Tris-HCl (pH 8.0) supplemented with oxaloacetate (0.6 mM) and NADH (0.2 mM). The oxidation of NADH was followed at 25 °C by measuring the decrease in absorbance at 340 nm using a Beckman DU 7500 spectrophotometer.

(2) Temperature-Dependent Enzymatic Assay. The measurements were carried out at a protein concentration of 20 μg/mL in a 1 cm thermostated cuvette containing 1 mL of 4 M NaCl, 0.2 mM NADH, and 0.6 mM oxaloacetate. The solutions were buffered with 50 mM Tris-HCl (pH 8) or 50 mM sodium cacodylate-HCl (pH 7). When the enzymatic assay was performed at lower NaCl concentrations, it was necessary to adapt the oxaloacetate concentration, according to its K_M dependence on the NaCl concentration (*42*). To maintain saturating conditions, the oxaloacetate concentrations were 0.1, 0.3, and 0.4 mM for 1.0, 2.0, and 3.0 NaCl, respectively.

Enzyme Deactivation. All the experiments were performed with protein stock solutions diluted 100-fold under the desired salt and buffer conditions. The final protein concentration was then about 0.1 mg/mL. After the desired incubation, the residual activity of the solution was measured in the standard buffer defined above. Results were expressed as the percentage of the activity relative to the enzyme maintained in 4 M NaCl.

(1) Effect of Salt Concentration. Samples at 25 °C were incubated at various salt concentrations for 24 h, and their residual activities were measured in the standard assay. The solutions were buffered with 50 mM Tris-HCl (pH 8) or 50 mM sodium cacodylate-HCl (pH 7).

(2) Effect of Temperature. Samples were incubated in 4 M NaCl and 50 mM Tris-HCl (pH 8) for 30 min at the indicated temperature, and their residual activities were measured. To avoid evaporation at high temperatures, the samples were covered with paraffin oil.

(3) Effect of pH. Samples were incubated in 4 M NaCl at 25 °C for 24 h, and their residual activities were measured in the standard assay. The different pH values were obtained by using the following buffers: 50 mM Tris-HCl (pH 8), 50 mM sodium cacodylate-HCl (pH 7), 50 mM sodium phosphate (pH 6), or 50 mM sodium citrate (pH 5) (*43*).

Small-Angle Neutron Scattering. A concentrated protein sample of the mutant was extensively dialyzed at 4 °C, against 2 or 4 M NaCl and 50 mM Tris (pH 8.2), in H_2O and diluted with the dialysate in 0.100 cm quartz cuvettes

to obtain three protein concentrations in the 5−20 mg/mL range. A fourth point at 28 mg/mL was measured only at 4 M NaCl. Neutron scattering experiments were performed at the Institut Laue Langevin (Grenoble), on the D11 instrument, using two sets of wavelength-collimation distance−sample−detector distance data: 10 Å−2 m−2.8 m, and 7 Å−4.0 m−4.5 m. The detector was moved to 1.2 m to measure the background intensities scattered at larger angles, to verify that the scattering of the buffer was properly subtracted. The data were treated in a standard way, by subtracting the scattering of the buffer cuvette and dividing by that of 0.100 cm of water (H_2O) and calibrated by using the procedure described in ref *44*. The square of the apparent radius of gyration ($R_{g_{app}}^2$) and the forward intensity $I(0)/c_2$ (c_2 is protein concentration) were obtained from Guinier plots [ln $I(Q)$ vs Q^2] in a $R_{g_{app}}Q$ range of 0.3−1.3 ($Q = 4\pi \sin\theta/\lambda$, with θ equal to half the scattering angle) (*45*). Coefficients describing the interparticle effect can be calculated from the dependence of $I(0)/c_2$ on c_2 (eq 5, below). The $I(0)/c_2$ and $R_{g_{app}}^2$ values were extrapolated to zero protein concentration to correct for interparticle effects (eq 5) and to obtain the mean square radius of gyration (R_g^2) and forward scattered intensity corresponding to the particles in solution. The extrapolated forward scattered intensity is related to the molar mass, M_2.

$$[I(0)/c_2]_{c_2=0} = M_2(\partial\rho_N/\partial c_2)_\mu^2/N_A \quad (1)$$

where N_A is Avogadro's number and $(\partial\rho_N/\partial c_2)_\mu$ is the neutron scattering length density increment expressing the contrast between the particle and the solvent (*44*). When the solution contains different types of particle (e.g., tetramers and dimers), R_g^2 and $[I(0)/c_2]_{c_2=0}$ correspond to weighted mean values that can be calculated from a model providing the relative concentrations of the different particles (*45*). For each solvent condition, $I(0)_{norm}/c_2$ values were calculated by normalizing the forward scattered intensity to 1.00 for the molar mass and contrast corresponding to the *Hm* MalDH tetramer. For practical reasons, measurements were performed at 4 °C for the wild type protein and 20 °C for the mutant. A control experiment on the wild type showed essentially identical results at the two temperatures.

Sedimentation Velocity. Sedimentation velocity experiments were performed using samples diluted from a stock solution stored at 4 °C in 4 M NaCl (pH 8.2). Experiments were performed in a Beckman XLA analytical ultracentrifuge, equipped with a UV scanning system, using a four-hole AN-60 Ti rotor with double centerpieces with 1.2 and 0.3 cm path lengths. In a typical experiment, 30 absorbance profiles for each sample were recorded after a suitable delay at 44 000 rpm. The delay (60−240 min) and wavelength were chosen according to the characteristics of the samples. The radial or time derivatives (*47*) of the profiles were analyzed using software provided by Beckman. The derivative profiles showed, unless otherwise mentioned, a symmetrical peak, the position of which was used to calculate the experimental sedimentation coefficient s_{exp} considered below as a weight average value. The corrected coefficients, s_{20w}, were calculated using tabulated viscosity η and density ρ, and apparent specific volumes φ deduced from experimental density increments $(\partial\rho/\partial c_2)_\mu$ (*48*).

$$(\partial\rho/\partial c_2)_\mu = 1 - \rho\varphi \quad (2)$$

$$s_{20w} = s_{exp}\{[(1 - \rho_{w,20}\varphi)/(1 - \rho\varphi)]\eta/\eta_{w,20}\} \quad (3)$$

Determination of the Association Constants. The equilibrium constants, K_a, were determined from the concentration dependence of the measured sedimentation coefficients, $s_{20,w}$, according to eq 4.

$$s_{20,w} = (1 - gc_2)(c_{dim}s_{dim} + c_{tetra}s_{tetra})/c_2 \quad (4)$$

$$c_{dim} + c_{tetra} = c_2$$

$$K_a = c_{tetra}/c_{dim}^2$$

where $s_{20,w}$ are weight average values over the different particles in the solution, c_2 is the total protein concentration, c_{dim} and c_{tetra} are the concentrations in the dimer and tetramer, respectively, and s_{dim} and s_{tetra} are the sedimentation coefficients at infinite dilution of the dimer and tetramer, respectively. The concentrations are given in units of grams per liter, and the factor g accounts for the interparticle effect. The value used for g was 0.008 L/g as determined for the wild type at 4 °C in either 2 or 4 M NaCl from the concentration dependence of the forward intensity in the neutron scattering experiments:

$$I(0)_{norm}/c_2 = (1 - gc_2)[I(0)_{norm}/c_2]_{c_2=0} \quad (5)$$

Size-Exclusion Chromatography. One hundred microliters of purified protein (5 mg/mL) was applied to a Superose 12 HR 10/30 (Pharmacia) column equilibrated at 25 °C in 4 M NaCl buffered at various pH values using 50 mM Tris-HCl (pH 8), 50 mM sodium cacodylate-HCl (pH 7), or 50 mM sodium phosphate (pH 6). A flow rate of 0.2 mL/min was maintained by means of the FPLC pump (Pharmacia). The elution profile was monitored by the absorbance at 280 nm, and the fractions were tested for specific activity in the standard enzymatic assay.

Fluorescence Experiments. Fluorescence measurements were carried out in a thermostated Aminco Bowman Series 2 luminescence spectrometer. For the intrinsic fluorescence measurement, a protein concentration of 20 μg/mL was used and the spectra were recorded between 300 and 450 nm at 20 °C in a 1 cm thermostated cuvette with an excitation wavelength of 280 nm and an integration time of 1 min. For the ANS fluorescence measurement, the spectra were recorded between 420 and 600 nm at 20 °C in a 1 cm thermostated cuvette with an excitation wavelength of 400 nm and an integration time of 1 min. The ANS concentration was 1 mM. All spectra were corrected for buffer.

The kinetic measurements of intrinsic fluorescence were performed on aliquots of different samples, each incubated at a given temperature, at regular time intervals. The amplitude of the fluorescence peak at 328 nm corresponding to maximal fluorescence for halophilic R207S/R292S MalDH, before incubation, was taken as 100%.

Circular Dichroism Spectroscopy. A Jobin Yvon CD6 circular dichroism spectropolarimeter with a thermostated sample holder was used. Data were recorded at 25 °C with an interval of 1 nm and an integration time of 15 s using very narrow cells (0.01 cm) because of the strong absorption by the high NaCl concentration. The protein concentration

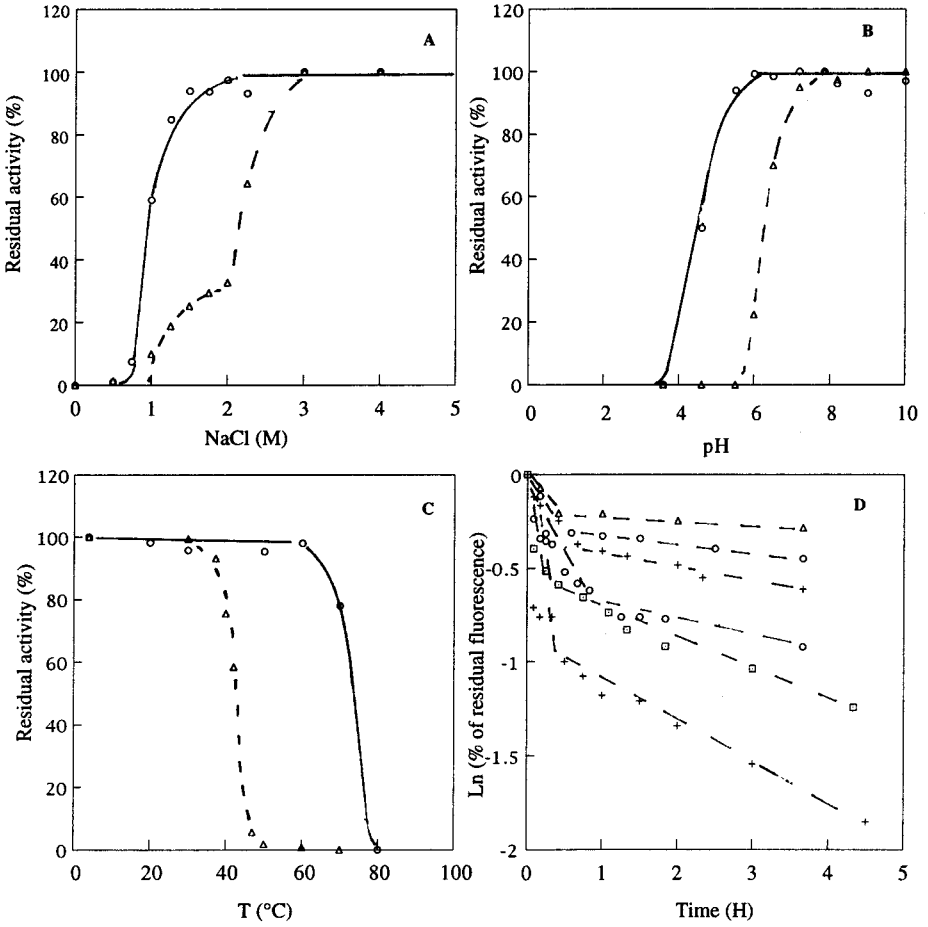

FIGURE 1: Deactivation of the wild type and R207S/R292S mutant of *Hm* MalDH under various conditions. (A and B) The extents of salt concentration-dependent deactivation at pH 8 in NaCl and the pH-dependent deactivation in 4 M NaCl were measured by the residual activity of R207/R292 *Hm* MalDH (△) and of wild type *Hm* MalDH (○) after incubation for 24 h at 20 °C. (C) The extent of thermal-dependent deactivation for both enzymes was measured after incubation for 30 min in NaCl (pH 8). (D) Kinetics of unfolding of R205S/R291S *Hm* MalDH at various temperatures measured by the decrease in intrinsic fluorescence at 328 nm: 32 (△), 36 (○), 38 (+), 44 (○), 46 (□), and 49 °C (+).

was 3 mg/mL at various NaCl concentrations buffered with 50 mM Tris-HCl (pH 8). Each spectrum is an average of three scans, corrected for buffer.

RESULTS

Effect of the Mutation on Stability. R207S/R292S *Hm* MalDH requires higher salt concentrations than the wild type for equivalent residual activity (Figure 1A). As previously reported, the salt-dependent transition between active and inactive species is strongly cooperative for the wild type enzyme (*37*, *39*). In contrast, the transition for the mutant was found to be biphasic at pH 8 in NaCl (Figure 1A) and in KCl (not shown), indicating the presence of inactivation intermediates in the solvent salt concentration range of 1−2 M. The transition was also studied by observing the fluorescence intensity of the protein under the same conditions. The data (not shown) reflect shifts in fluorescence maxima that can be strictly superimposed on the residual activity curves. These are discussed further below.

Compared to that of the wild type enzyme, the pH-dependent deactivation of R207S/R292S *Hm* MalDH in 4 M NaCl was shifted by 2 pH units (Figure 1B).

The mutations also induce a strong change in the thermal deactivation of the protein, which starts at 35 °C, whereas the wild type is stable up to 60 °C (Figure 1C). The temperature for which the enzyme loses 50% of its residual activity in 30 min is lowered from 75 °C for the wild type to 45 °C for the mutant. In 4 M NaCl (pH 8), the kinetics of unfolding of the mutant was measured by following the fluorescence emission during incubation at various temperatures (Figure 1D). The process was found to be biphasic between 35 and 48 °C, while the thermal deactivation kinetics of the wild type protein is first-order (*41*).

In the case of wild type *Hm* MalDH, loss of activity at low salt concentrations has been shown to be directly correlated with dissociation and concomitant unfolding (*38*, *40*). Residual activity measurements, in general, can be related to kinetic and/or equilibrium processes affecting enzyme stability. The residual activity experiments with R207S/R292S *Hm* MalDH suggested that it exists as different folded species depending on experimental conditions, and biophysical experiments were then performed to monitor the molar mass and structure of each species.

Small-Angle Neutron Scattering Identified Three Different Species. In 4 M NaCl (pH 8) and for the protein concentration range above 5 mg/mL, the R207S/R292S *Hm* MalDH is predominantly a tetramer with a radius of gyration (R_g) of 30 Å, identical to the one measured previously for the wild type protein (*48*). The normalized forward scattered neutron intensity, however, was slightly lower than that for the wild

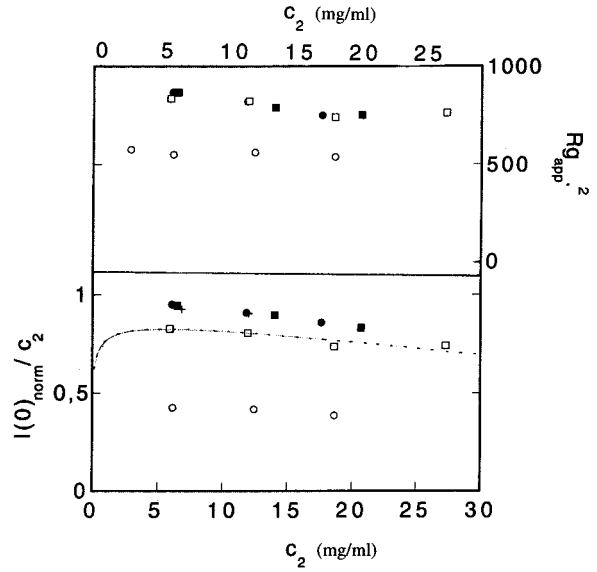

FIGURE 2: Neutron scattering characterization of wild type and R207S/R292S *Hm* MalDH. The square of the apparent radius of gyration, $R_{g_{app}}{}^2$, and forward intensity, $I(0)_{norm}/c_2$ (proportional to the molar mass and normalized to 1.00 for the protein tetramer at infinite dilution in each contrast condition), obtained from Guinier plots are plotted as a function of protein concentration, c_2, for the wild type (black symbols) and the R207S/R292S mutant (white symbols) in 4 M NaCl (squares) and 2 M NaCl (circles). The dotted line is calculated using both neutron scattering and sedimentation data, considering a dimer−tetramer equilibrium with interparticle effects and an association constant of 1.3×10^5 M^{-1} in 4 M NaCl (see Materials and Methods).

type, indicating mild dissociation. It could be modeled very well in terms of a tetramer−dimer equilibrium, with association constants comparable with those found in the sedimentation experiments (see below) (Figure 2).

At 2 M NaCl, an R_g of 24 Å was measured for the R207S/R292S *Hm* MalDH. This value is much lower than the value of 30 Å obtained in 4 M NaCl. On the other hand, the R_g of the wild type MalDH is the same in 2 and 4 M NaCl. The normalized forward scattered intensity of the mutant in 2 M NaCl was lower by a factor of 2 when compared to that of the wild type under similar conditions (Figure 2), clearly indicating that the mutant is a dimer under these conditions. The experimental R_g of 24 Å found for the mutant in 2 M NaCl is close to the value of 25 Å, calculated for a hypothetical dimer from the coordinates of the crystallographic structure of *Hm* MalDH (*49*). This value is also very close to 23 Å, the R_g of the dimeric cytoplasmic pig MalDH (*48*). Addition of NADH has been found to increase the half-life of dissociation of halophilic wild type MalDH at low NaCl concentrations (*38*). In a SANS experiment, addition of 2.5 mM NADH to R207S/R292S *Hm* MalDH in 2 M NaCl (pH 8) did not modify its association state. The mutant remained in the dimeric form.

Another species with smaller dimensions ($R_g = 20$ Å) than the dimer was detected in a single SANS experiment performed at 5 mg/mL in 4 M NaCl (pH 8) after incubation for 15 min at 40 °C. The R_g value of the tetrameric wild type protein was not sensitive to this temperature jump and remained constant. The value of 20 Å is close to the theoretical value of 19 Å calculated from the crystal structure for a compact folded monomer. After incubation for 2 h at this temperature, the mutant protein was totally precipitated. The monomer was not formed in the presence of NADH. Upon addition of 2.5 mM NADH at 40 °C in 4 M NaCl (pH 8), a constant R_g value of 30 Å was found for the mutant, showing the protein remains tetrameric.

Salt and pH-Dependent Structural Changes Monitored by Sedimentation Velocity Experiments. Analytical ultracentrifugation (AUC) was used to investigate the structural properties of the mutant in a protein concentration range that was lower than that studied by SANS. Panels A and B of Figure 3 present the distribution functions of the sedimentation coefficient for R207S/R292S *Hm* MalDH in 4 and 2 M NaCl, respectively. In 4 M NaCl, a symmetrical peak was found, which shifted to larger *s* values with higher protein concentrations. In 2 M NaCl, the profiles superimpose for the various protein concentrations, and some slow sedimenting material was detected. The amount of this slow species increased significantly when the incubation time was increased. The corrected $s_{20,w}$ coefficients for the major peak are presented in Figure 3C. The $s_{20,w}$ measured for the wild type protein in 4 M NaCl was 6.7 S, corresponding to the tetramer (data not plotted). The $s_{20,w}$ value found at the lower protein concentration of R207S/R292S *Hm* MalDH in 4 M NaCl was the same as found in 2 M NaCl. These results can be fitted reasonably well by a dimer−tetramer equilibrium (dotted lines). The reversibility of this salt-induced dimer−tetramer equilibrium for the mutant was investigated by preparing a 3 mg/mL protein sample that was incubated for 1 h in 2 M NaCl and diluted with 5 M NaCl to 4 M NaCl prior to centrifugation. The *s* values measured for this sample were identical to those at 4 M NaCl without prior incubation at the lower salt concentration. From the SANS and AUC results, equilibrium constants of 1.3×10^5, 1.6×10^4, 2.6×10^3, and 3.2×10^2 M^{-1} were calculated for the dimer−tetramer association in 4, 3, 2.5, and 2 M NaCl, respectively. For these calculations, an $s_{20,w}$ value of 4.3 S (corresponding to the mutant in 2 M NaCl) was used for the dimer; an $s_{20,w}$ value of 6.7 S was used for the tetramer. We note that the $s_{20,w}$ value found for the dimeric *Hm* MalDH in 2 M NaCl is very close to the value obtained for the dimeric intermediate of LDH ($s_{20,w} = 4.2$ S) upon dissociation of the tetrameric protein following incubation in 1 M guanidinium chloride (*16*).

The pH-dependent dissociation of the mutant was monitored at high salt concentrations. The data shown in Figure 3D indicated that the hydrodynamic properties of the mutant are the same in 4 M NaCl buffered at pH 8 or 7. The mutant clearly remains a dimer ($s_{20,w} = 4.3$ S) at low protein concentrations (50 μg/mL), whereas at pH 6, the $s_{20,w}$ value decreased to 2.2 S, suggesting dissociation into monomers.

Fluorescent Properties of R207S/R292S Hm MalDH. There are two tryptophans per monomer in the structure of the enzyme, located at the intersubunit regions (*30*, *31*). Changes in their solvent accessibility upon dissociation were expected to be correlated with changes in the fluorescent properties of the protein. Fluorescence spectra were therefore recorded for low protein concentrations under conditions where the dimeric [4 M NaCl (pH 7 or 8)] or the monomeric species [4 M NaCl (pH 6)] of R207S/R292S *Hm* MalDH were observed by AUC. The maximum of the fluorescence emission of the tetrameric wild type enzyme, centered at 332 nm, is shifted to 328 nm for the mutant dimer (Figure 4A). The 4 nm red shift and the decrease in the maximum of

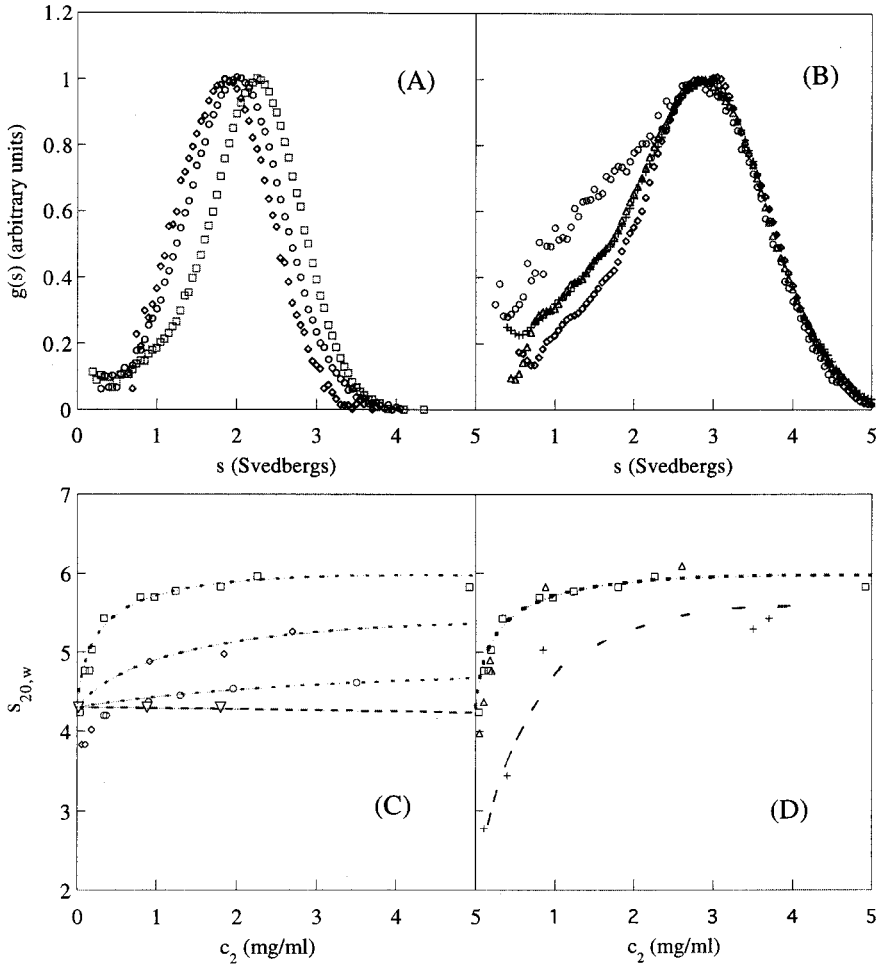

FIGURE 3: Sedimentation velocity experiments on R207S/R292S *Hm* MalDH. (A) Effect of R207S/R292S *Hm* MalDH concentration on the sedimentation coefficient distribution, $g(s)$, in 4 M NaCl at 20 °C. The loading protein concentrations are 0.15 (◇), 0.3 (○), and 2 mg/mL (□). (B) In 2 M NaCl, at 0.05 (○), 1 (△), and 2 mg/mL (◇). The crosses correspond to a 1 mg/mL sample incubated for 24 h at 20 °C. (C) Effects of NaCl concentration with the corrected sedimentation coefficients of the R207S/R292S mutant derived from the major peak at 20 °C in 4 M (□), 3 M (◇), 2.5 M (○), and 2 M NaCl (▽). (D) Effect of pH at 20 °C: pH 8.2 (□), 7 (△), and 6 (+). The dotted lines in panels C and D are calculated using both neutron scattering and sedimentation data considering a dimer−tetramer equilibrium with a correction for interparticle effects (see Materials and Methods). The dashed line in panel D is to guide the eye through the points for the pH 6 data.

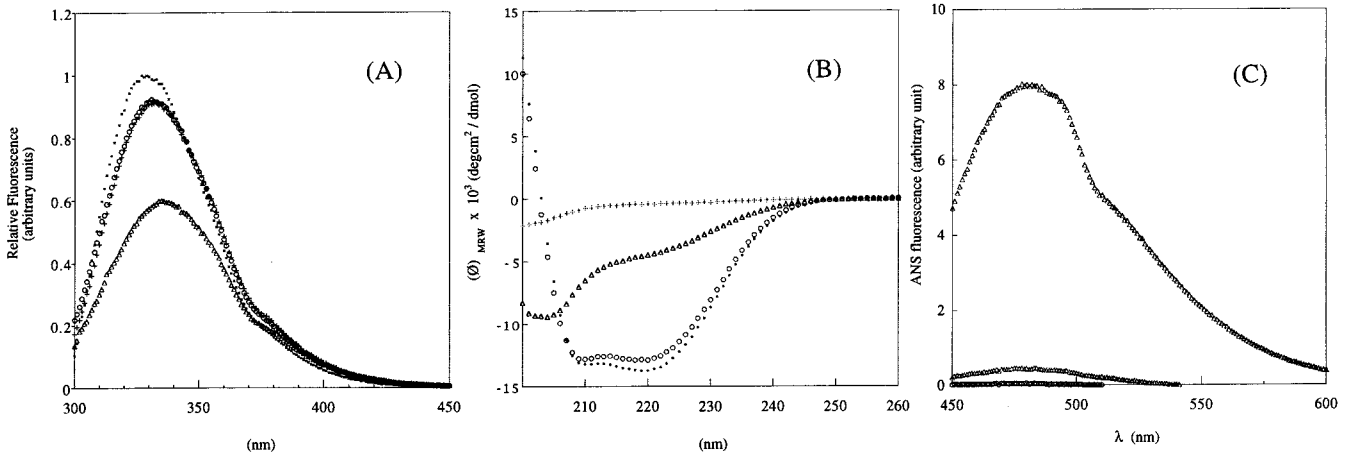

FIGURE 4: Spectral properties of R207S/R292S *Hm* MalDH. (A) Intrinsic fluorescence of R207S/R292S *Hm* MalDH in 4 M NaCl buffered at pH 6 (△), 7 (+), or 8 (○) and of wild type *Hm* MalDH (×). The protein concentration was 20 mg/mL. (B) Far-UV circular dichroism spectra of R207S/R292S *Hm* MalDH recorded at 20 °C in 4 M NaCl at pH 8 (●), 2 M NaCl at pH 8 (○), 2 M NaCl at pH 8 after incubation at 45 °C for 10 min (△), and 0 M NaCl at pH 8 after incubation for 24 h at 20 °C (+). (C) Effect of temperature on the 1-anilinonaphthalene-8-sulfonate fluorescence of R207S/R292S *Hm* MalDH at 20 °C in 4 M NaCl at pH 8 and (▽) 4 M NaCl at pH 8 and 40 °C (△) and wild type *Hm* MalDH at 20 °C in 4 M NaCl at pH 8, (○).

fluorescence emission suggest that W304 that is located in the dimer−dimer interface, and becomes more solvent-exposed upon dissociation into dimers. The other tryptophan, W247, faces its counterpart on an adjacent monomer across

a symmetry axis in the tetramer. This residue is also involved in hydrophobic stacking with Y38 of the adjacent monomer. The strong decrease in the fluorescence and the shift at 335 nm when the spectrum was recorded at 4 M NaCl (pH 6) (a condition that was shown to cause the dissociation of the mutant enzyme to monomers) are in accordance with partial solvent exposure of W247 upon dissociation into monomers. The emission spectra of the unfolded monomers, obtained after incubation for 24 h at 0.05 M NaCl (pH 8) for either the mutant or the wild type protein, were identical, with an emission maximum at a higher wavelength (350 nm) and a lower intensity (*7*) (data not shown).

Combining the fluorescence spectra results presented above with the residual enzymatic measurements shown in Figure 1A suggests that the stable dimeric form (above 2 M NaCl) is active.

Secondary Structure Content of R207S/R292S Hm MalDH. In 4 M NaCl (pH 8) and 2 M NaCl (pH 8), the far-UV CD spectrum recorded at 3 mg/mL R207S/R292S *Hm* MalDH exhibited a broad negative dichroism band centered at 210−220 nm, with an amplitude of $\geq$15000 deg cm^2 dmol^{-1}, very similar to spectra observed for the wild type enzyme and LDH (*51*) (Figure 4B). The overall secondary structure content of the tetramer or the dimer therefore is not modified by the mutation. The spectrum of the mutant obtained after incubation for 24 h in 0.05 M NaCl is typical of the fully unfolded form, showing no secondary structure. The CD spectrum recorded under conditions similar to those where the species with an R_g of 20 Å was detected by SANS [4 M NaCl (pH 8), incubation at 45 °C for 10 min] indicates that the monomeric species has less secondary structure than the dimer or tetramer.

The Dimer Exists in Active and Inactive Forms Depending on the pH. The respective activities of the wild type and R207S/R292S *Hm* MalDH were measured in the standard enzymatic assay buffered at pH 8 at various NaCl concentrations and protein concentrations (<50 μg/mL) where the mutant was shown by analytical centrifugation to be dimeric. The catalytic velocities (millimoles of NADH consumed per minute per milligram) of both enzymes were found to be identical between 4 and 2 M NaCl. The data recorded at 4 M NaCl are presented (Figure 5A,B). The mutant displays its maximum activity at 60 °C, the same temperature as for the wild type protein (*52*). Moreover, this temperature is independent of the salt concentration for both wild type and mutant enzymes. Strikingly, a substantial loss of activity for the R207S/R292S *Hm* MalDH was observed when the standard enzymatic assay was performed at pH 7 (Figure 5B). Weak enzymatic activity of the mutant was detected only when the temperature of the assay reached 60 °C. The enzymatic activity of wild type *Hm* MalDH, however, was identical at pH 7 and 8. To achieve a better understanding of this pH-dependent inactivation, the following experiment was designed. The respective fluorescent spectra of the wild type and mutant protein were recorded at 25 °C in the reaction mixtures (in 4 M NaCl, at various pH values) before addition of the coenzyme, and then the NADH was added to the mixtures. As has been described for LDH (*53*), the addition of NADH strongly quenches the intrinsic fluorescence of both enzymes. Excess NADH gives a signal at 450 nm (Figure 5C,D). At pH 8, when oxaloacetate was added to the samples, oxidation of all the NADH occurred very rapidly (<1 min), and because NAD^+ does not stay bound or have a quenching effect in solution, the intrinsic fluorescence of the apoprotein was restored (Figure 5C). At pH 7, however, this was true only for the wt enzyme and not the case for the mutant (Figure 5D). Even after a long incubation at pH 7, the NADH still quenched the intrinsic fluorescence of the mutant, confirming that under these conditions the enzyme is inactive. Since it was shown that the mutant does not dissociate into monomers at pH 7, the results suggest that even if the dimeric R207S/R292S *Hm* MalDH is able to bind the coenzyme, it remains in a noncatalytic state.

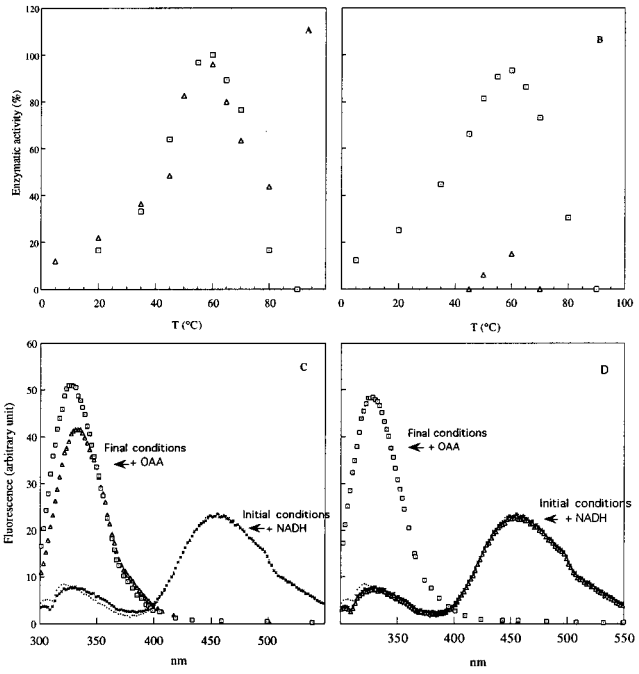

FIGURE 5: Thermal-dependent enzymatic activity of R207S/R292S *Hm* MalDH (△) and wild type *Hm* MalDH (□). The solution was buffered at pH 8 (A) and 7 (B). The data were corrected for thermal oxidation of NADH. The results are expressed as a percentage of the maximal velocity, which was identical for both enzymes. (C and D) Effect of NADH and oxaloacetate addition on the intrinsic fluorescence of R207S/R292S and wild type *Hm* MalDH in 4 M NaCl at pH 8 or 7. The spectra were recorded at 20 °C. After addition of 50 mM NADH to samples, spectra for R207S/R292S *Hm* MalDH (×) and wild type *Hm* MalDH (●) were recorded between 300 and 550 nm. After addition of 50 mM oxaloacetate to the previous samples, the fluorescence spectra were rescanned for R207S/R292S *Hm* MalDH (△) and wild type *Hm* MalDH (□).

8-Anilinosulfonate (ANS) Binding to R207S/R292S Hm MalDH. At room temperature, in 4 M NaCl (pH 8), ANS did not bind to the tetrameric wild type *Hm* MalDH, and only a very low ANS fluorescence intensity was detected for R207S/R292S *Hm* MalDH in the dimeric state (Figure 4C). The ANS fluorescence intensity of each of the wild type and mutant proteins was also recorded at low protein concentrations under conditions of thermal deactivation (not shown). For the mutant, the fluorescence increased between 35 and 45 °C and decreased at higher temperatures. For the wild type, these variations started at a higher temperature (75 °C) and with a 10-fold lower intensity. The monomeric state of R207S/R292S *Hm* MalDH obtained at low pH [in 4 M NaCl (pH 6)] was also able to bind ANS at 20 °C, with a spectrum similar to that of the high-temperature monomer (not shown). These results indicated that the monomeric structure obtained in the mutant, with either high temperature

or low pH, is less compact than the fully folded dimer or tetramer.

Reactivation of the Monomeric State. The presence of partially folded monomeric species of R207S/R292S *Hm* MalDH was detected also by size-exclusion liquid chromatography using Superose 12HR (not shown). When equilibrated with 4 M NaCl buffered at pH 8, 7, or 6, the elution volume (V_e) of the tetrameric wild type *Hm* MalDH was found to be 9.8 mL under all conditions. On the other hand, the elution volume for the mutant was shifted to 12.6 mL at pH 6, suggesting a monomeric state, whereas it was the same for the wild type at the higher pH values. This confirmed the dissociation into monomers observed also by AUC in 4 M NaCl (pH 6). It has been shown that size-exclusion liquid chromatography was a good method for separating folding intermediates, including molten globule states (*54*). The properties (λ_{max} of intrinsic fluorescence at 335 nm and ANS binding) of the purified monomeric species eluted from the column at 12.6 mL were found to be similar to those previously observed. The monomeric species was found to be enzymatically inactive under the standard conditions during the time of the assay (less than 1 min). When the NADH oxidation was recorded for a longer period of time (10 min), however, it was possible to detect some activity. The initial rate of the reaction increased with time, suggesting a continuous reactivation induced by the components of the standard enzymatic buffer. When the protein concentration was raised, the reactivation occurred more rapidly. Either NADH or Tris-HCl buffer (pH 8), therefore, fully restored enzymatic activity to the monomeric fractions.

DISCUSSION

Properties of the Monomer. Measurements of ANS fluorescence intensity are commonly applied to detect molten globule intermediates upon protein folding or unfolding (*53*−*55*). The monomer of *Hm* MalDH has the ability to bind ANS, and its far-UV CD spectrum shows reduced secondary structure. These are properties of a molten globule-like structure. Of the criteria defining this state (*58*), only the absence of tertiary interactions was not established. This is usually observed in the near-UV CD spectrum, which could not be determined for the *Hm* MalDH monomer because of the strong light absorption induced by the high NaCl concentration in the samples. The monomeric intermediate aggregates and precipitates at protein concentrations higher than about 1 mg/mL, probably because of its nonpolar surface area. The rate of fluorescence change of the mutant protein exhibited biphasic behavior as a function of temperature, which can be interpreted as dissociation of the dimer followed by unfolding of the monomer. A two-step process had also been observed for the thermal inactivation of the dimeric mitochondrial pig MalDH, immobilized via one protomer on Sepharose beads, and interpreted as a rapid dissociation of the dimer followed by a slower inactivation of the Sepharose-bound monomeric unit (*59*).

Whether or not the MalDH monomer is active has been a subject of controversy (*60*−*62*). A stable monomeric unit of *Escherichia coli* MalDH has been constructed by protein engineering and demonstrated to be inactive (*63*). It is difficult to establish if the monomeric intermediate of *Hm* MalDH is slightly active, because the addition of NADH coenzyme has been shown to reactivate the enzyme, probably by inducing dimerization. An electrostatic calculation on the *Hm* MalDH structure has shown strong pK_a shifts for catalytic residues upon dissociation into monomers, which would be incompatible with enzymatic activity (*64*). We propose, therefore, that the *Hm* MalDH monomer is in an inactive "molten globule-like" state, which can be reactivated through a structural change induced by NADH binding that allows it to associate into active dimers.

Properties of the Dimer. A pH-dependent deactivation of tetrameric MalDH has been observed for two species of *Bacillus*. The MalDH from *Bacillus subtilis* is reversibly inactivated at pH 8 to form monomers, with no observable intermediates. The enzyme from *Bacillus israeli*, on the other hand, dissociates into dimers at pH 3.5, but it is not clear if they are enzymatically active (*10*, *65*). In wild type *Hm* MalDH, the salt-dependent deactivation is significantly modified by a pH shift between 7 and 8; at a constant salt concentration, the protein is markedly more stable at pH 8 (*66*). We suggest that this effect is probably related to the pH-dependent stability and activity of the dimeric intermediate, which, in the wild type, is very unstable under low-salt conditions. The mutation, on the other hand, stabilizes the dimer sufficiently so that it can be observed and studied. R207S/R292S *Hm* MalDH dissociates into dimers at 2 M NaCl, or at very low protein concentrations in 4 M NaCl above pH 7. This dimer is as active as the wild type tetramer at pH 8 but loses its activity at pH 7, without large changes in structure or association state. The intrinsic fluorescence, far-UV CD spectrum, and $s_{20,w}$ values remain identical at pH 7 and 8. The switch between an active and inactive dimer of R207S/R292S *Hm* MalDH, therefore, is likely to be due to a change in the ionization state of a critical active site residue with a p*K* value between 7 and 8. Dimeric mitochondrial MalDH also displays a reversible pH-dependent dissociation into monomers, related to the ionization state of a histidine residue (H68), located at the monomer−monomer interface within the dimer (*60*, *61*, *67*). H68 is involved in dimer stabilization, but it also interacts with an important catalytic residue in the adjacent subunit, which takes part in substrate binding (*68*). The 2.6 Å resolution structure of *Hm* MalDH shows the H68 equivalent residue is also involved in intersubunit contacts in the dimer and interacting with R171 in the catalytic site of the adjacent monomer (*31*). R171 contributes to substrate binding and recognition and is strictly conserved in all MalDHs and LDHs (*24*). If H68 is responsible for the pH inactivation of the dimeric R207S/R292S *Hm* MalDH, then other interactions must be invoked to stabilize the dimer structure, which, in contrast to mitochondrial MalDH, is maintained during this transition. This suggested that there are subtle differences at the monomer−monomer interface between tetrameric (LDH-like) and dimeric (e.g., mitochondrial) MalDH. We note that of the two different possible dimers in the LDH-like tetramer [AB−DC or AD−BC (*31*)], only the one discussed in this paper (AB−DC) can be enzymatically active. The catalytic site residues of the AD−BC dimer would not have the correct ionization state (*64*).

Dimers have been observed previously for some bacterial LDHs, but they are only weakly active (*16*, *17*, *69*, *70*). The dimer−dimer interface in these enzymes is such that the binding of an allosteric activator controls tetramer oligo-

merization and activity, whereas this property has not been observed for a tetrameric MalDH. The *Hm* MalDH dimeric intermediates have, depending on the conditions, activity properties that are similar either to those of the LDH dimeric intermediates or to those of the dimeric MalDH enzyme families.

Mechanisms That Favor and Maintain the Tetrameric State. Our results showed that the *Hm* MalDH tetramer can be considered as an association of two active dimers. In dimeric MalDH enzymes, such as pig mitochondrial MalDH, tetramer formation appears to be prevented by steric clashes between large loops from adjacent monomers (*71*). A stable, inactive dimer of LDH from *B. stearothermophilus* has been constructed by a four-residue insertion in one of these loops, thereby supporting the hypothesis that a longer loop prevents association into tetramers (*71*). Comparisons of the sequences and three-dimensional structures of tetrameric *Hm* MalDH (*31*), mitochondrial pig heart MalDH (*35*), and *Squalus acanthias* LDH (*72*) show that the loop in *Hm* MalDH has an additional six-residue deletion and the omission of a secondary structure element compared with tetrameric LDH, thus positioning two aspartic residues (D209 and D211) involved in complex salt bridge clusters across the dimer−dimer interface (*31*). A second clash is also abolished in *Hm* MalDH, the loop being similar to LDH, whereas it is four residues longer in dimeric MalDH. The *Hm* MalDH structure, however, is the only one available so far for a tetrameric MalDH, and it is not clear which characteristics correspond to general properties of the [LDH-like] MalDH and which are specific to halophilic adaptation. In the wild type protein, the Arg residues contribute strongly to the stabilization of the tetramer, because of their particularly favorable structure for complex salt bridge formation. Arg residues have in fact been seen to play pivotal roles in ionic network stabilization of interface interactions in hyperthermophilic proteins (*73*). Solvent−protein interactions have not been discussed, previously, with respect to oligomerization of LDH. The novel solvent interactions observed in the crystallographic structure of *Hm* MalDH (*31*), however, appear to play an essential role and help us understand that even with the disrupted intramolecular salt bridges, the recombinant protein remains a tetramer at high NaCl concentrations.

Bridging the Gap between LDH and MalDH. The study presented here shows that the active mutant of *Hm* MalDH dissociates under certain conditions to active dimers and under other conditions to inactive dimers. These dimers further dissociate into folded monomers which eventually unfold. It was demonstrated previously that wild type *Hm* MalDH can be reactivated from monomers with second-order kinetics (*7*, *52*), which implies that dimeric intermediates should exist also in the wild type *Hm* MalDH. Combining these results with the folding and association pathways of L-LDH and dimeric MalDH (*17*) suggests a general mechanism:

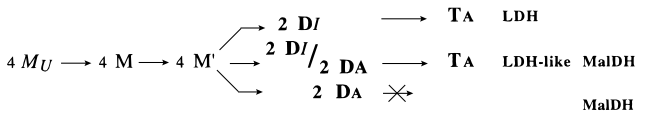

M_U is the unfolded chain; it folds into an inactive monomeric species M that can undergo a conformational change to a species M′, which condenses into dimers D. Once the dimeric species is formed, the various enzymatic states (active A and inactive *I*) observed for halophilic LDH-like MalDH allow us to establish a subtle evolutionary divergence between LDH (inactive dimers) and active dimeric MalDH (cytoplasmic and mitochondrial). The molecular contacts between active dimers that take place in the formation of tetramers, T, are forbidden due to steric clashes at the dimer−dimer interface.

ACKNOWLEDGMENT

Acknowledgments are due to Sebastien Courty and Stefania Nuzzo who performed part of the centrifugation and circular dichroism experiments during their "Maîtrise" placement in the laboratory, to O. Landman and V. Kotlyar for the site-directed mutagenesis, and to Géraldine Serre for her skillful technical help. Thanks are also due to Dr. W. Stafford for the generous gift of his analytical centrifugation software, to Dr. Anna Mitraki for a critical reading of the manuscript, and to Flavien Proust for help with the figures.

REFERENCES

1. Banaszak, L. J., and Bradshaw, R. A. (1975) Malate dehydrogenase. In *The Enzymes*, 3rd ed. (Boyer, P. D., Ed.) pp 369−396, Academic Press, New York.
2. Birkoft, J. J., Fernley, R. T., Bradshaw, R. A., and Banaszak, L. J. (1982) *Proc. Natl. Acad. Sci. U.S.A. 79*, 6166−6170.
3. Schar, H. P., and Zuber, H. (1979) *Hoppe-Seyler's Z. Physiol. Chem. 360* (7), 795−807.
4. Chaga, G., Andersson, L., and Porath, J. (1992) *J. Chromatogr. 627* (1−2), 163−172.
5. Tihanyi, K., Fontanell, A., Talbot, B., and Thirion, J. P. (1989) *Arch. Biochem. Biophys. 274* (2), 626−632.
6. Rolstad, A. K., Howland, E., and Sirevag, R. (1988) *J. Bacteriol. 170* (7), 2947−2953.
7. Mevarech, M., and Neumann, E. (1977) *Biochemistry 16*, 3786−3792.
8. Smith, K., Sundaram, T. K., and Kernick, M. (1984) *J. Bacteriol. 157*, 17−25.
9. Hartl, T., Grossebüter, W., Görisch, H., and Stezowski, J. J. (1987) *Biol. Chem. Hoppe-Seyler 368*, 259−267.
10. Wynne, S. A., Nicholls, D. J., Scawen, M. D., and Sundaram, T. K. (1996) *Biochem. J. 317*, 235−245.
11. Wilks, H. M., Hart, K. W., Feeney, R., Dunn, C., Muirhead, H., Chia, W. N., Barstow, D. A., Atkinson, T., Clarke, A., and Holbrook, J. J. (1988) *Science 242*, 1541−1544.
12. Nicholls, D. J., Miller, J., Scawen, M. D., Clarke, A. R., Holbrook, J. J., Atkinson, T., and Goward, C. R. (1992) *Biochem. Biophys. Res. Commun. 189* (2), 1057−1062.
13. Cendrin, F., Chroboczek, J., Zaccaï, G., Eisenberg, H., and Mevarech, M. (1993) *Biochemistry 32*, 4308−4313.
14. Wigley, D. B., Gamblin, S. J., Turkenburg, J. P., Dobson, E. J., Piontek, K., Muirhead, H. M., and Holbrook, J. J. (1992) *J. Mol. Biol. 223*, 317−335.
15. Chapman, A. D. M., Cortés, A., Dafforn, T. R., Clarke, A. R., and Brady, R. L. (1999) *J. Mol. Biol. 285*, 703−712.
16. Jaenicke, R., Vogel, W., and Rudolph, R. (1981) *Eur. J. Biochem. 114*, 525−531.
17. Jaenicke, R. (1998) Oligomeric proteins. In *Molecular chaperones in the life cycle of proteins* (Fink, A. L., and Goto, Y., Eds.) pp 35−70, Marcel Dekker, New York.
18. Clarke, A. R., Wigley, D. B., Barstow, D. A., Chia, W. N., Atkinson, T., and Holbrook, J. J. (1987) *Biochim. Biophys. Acta 913* (1), 72−80.
19. Wrba, A., Jaenicke, R., Huber, R., and Stetter, K. O. (1990) *Eur. J. Biochem. 188*, 195−201.
20. Chiou, S. H., Lee, H. J., Huang, S. M., and Chang, G. G. (1991) *J. Protein Chem. 10* (2), 161−166.
21. Iwata, S., Kamata, K., Yoshida, S., Minowa, T., and Otha, T. (1994) *Nat. Struct. Biol. 1* (3), 176−185.

22. Wigley, D. B., Gamblin, S. J., Turkenburg, J. P., Dodson, E. J., Piontek, K., Muirhead, H., and Holbrook, J. J. (1992) *J. Mol. Biol. 223* (1), 317−335.
23. Holbrook, J. J., Liljas, A., Steindel, S. J., and Rossmann, M. G. (1975) in *The Enzymes*, 3rd ed. (Boyer, P. D., Ed.) Vol. 11, pp 191−292, Academic Press, New York.
24. Sundaram, T. K., Wright, I. P., and Wilkinson, A. E. (1980) *Biochemistry 19*, 2017−2022.
25. Goward, R. C., and Nicholls, D. J. (1994) *Protein Sci. 3*, 1883−1888.
26. Naterstad, K., Lauvrak, V., and Sirevåg, R. (1996) *J. Bacteriol. 178*, 7047−7052.
27. Synstad, B., Emmerhoff, O., and Sirevåg, R. (1996) *Arch. Microbiol. 165*, 346−356.
28. Charnock, C. (1997) *J. Bacteriol. 179* (12), 4066−4070.
29. Langelandsvik, A. S., Steen, I. H., Birkeland, N. K., and Lien, T. (1997) *Arch. Microbiol. 168*, 59−67.
30. Dym, O., Mevarech, M., and Sussman, J. L. (1995) *Science 267*, 1344−1346.
31. Richard, S., Madern, D., Garcin, E., and Zaccaï, G. (2000) *Biochemistry 39*, 992−1000.
32. Birktoft, J. J., Rhodes, G., and Banaszak, L. J. (1989) *Biochemistry 28* (14), 6065−6081.
33. Hall, M. D., Levitt, D. G., and Banaszak, L. J. (1992) *J. Mol. Biol. 226* (3), 867−882.
34. Kelly, C. A., Nishiyama, M., Ohnishi, Y., Beppu, T., and Birktoft, J. J. (1993) *Biochemistry 32*, 3913−3922.
35. Gleason, W. B., Fu, Z., Birktoft, J., and Banaszak, L. (1994) *Biochemistry 33*, 2078−2088.
36. White, M. F., Fothergill, L. A., Kelly, S. A., and Price, N. C. (1993) *Biochem. J. 295*, 743−748.
37. Bailey, D. L., Fraser, M. E., Bridger, W. A., James, M. N. G., and Woloko, W. T. (1998) *J. Mol. Biol. 285*, 1655−1666.
38. Pundak, S., Aloni, H., and Eisenberg, H. (1981) *Eur. J. Biochem. 118*, 471−477.
39. Bonneté, F., Madern, D., and Zaccai, G. (1994) *J. Mol. Biol. 244*, 436−447.
40. Zaccai, G., Bunick, G. J., and Eisenberg, H. (1986) *J. Mol. Biol. 192*, 155−157.
41. Madern, D., Pfister, C., and Zaccai, G. (1995) *Eur. J. Biochem. 230*, 1088−1095.
42. Hecht, K., Wrba, A., and Jaenicke, R. (1989) *Eur. J. Biochem. 183*, 69−74.
43. Dawson, R., Elliott, D., Elliott, W., and Jones, K. (1968) *Data for Biochemical Research*, 2nd ed., Claredon Press, Oxford, U.K.
44. Jacrot, B., and Zaccai, G. (1981) *Biopolymers 20*, 2413−2426.
45. Zaccai, G., and Jacrot, B. (1983) *Annu. Rev. Biophys. Bioeng. 12*, 139−157.
46. Eisenberg, H. (1981) *Q. Rev. Biophys. 14*, 141−172.
47. Stafford, W. F. (1992) *Anal. Biochem. 203*, 295−301.
48. Bonneté, F., Ebel, C., Zaccaï, G., and Eisenberg, H. (1993) *J. Chem. Soc., Faraday Trans. 89*, 2659−2666.
49. Svergun, D., Barberato, C., and Koch, M. J. (1995) *J. Appl. Crystallogr. 28*, 768−773.
50. Calmettes, P., Eisenberg, H., and Zaccai, G. (1987) *Biophys. Chem. 26*, 279−290.
51. Rudolph, R., Heider, I., Westhof, E., and Jaenicke, R. (1977) *Biochemistry 16*, 3384−3389.
52. Hecht, K., and Jaenicke, R. (1989) *Biochemistry 28*, 4979−4985.
53. Holbrook, J. J., and Stinson, R. A. (1973) *Biochem. J. 131*, 739−748.
54. Uversky, V. N. (1993) *Biochemistry 32*, 13288−13298.
55. Ptitsyn, O. B., Pain, R. H., Semistonov, G. V., Zerovnik, E., and Razgulyaev, O. I. (1990) *FEBS Lett. 262*, 20−24.
56. Jones, B. E., Jennings, P. A., Pierre, R. A., and Matthews, R. (1994) *Biochemistry 33*, 15250−15258.
57. Biplab, K. D., Bhattacharyya, T., and Roy, S. (1995) *Biochemistry 34*, 5242−5247.
58. Kuwajima, K. (1989) *Proteins: Struct., Funct., Genet. 6*, 87−103.
59. Jurgensen, S. R., Wood, D. C., Mahler, J. C., and Harrison, J. H. (1981) *J. Biol. Chem. 256*, 2383−2388.
60. Bleile, D. M., Schulze, R. A., Harrison, J. H., and Gregory, E. M. (1977) *J. Biol. Chem. 252*, 755−758.
61. Wood, D. C., Jurgensen, S. R., Geesin, J. C., and Harrison, J. H. (1981) *J. Biol. Chem. 256*, 2377−2382.
62. McEvily, A. J., Mullinax, T. R., Dulin, D. R., and Harrison, J. H. (1985) *Arch. Biochem. Biophys. 238*, 229−236.
63. Breiter, D. R., Resnik, E., and Banaszak, L. J. (1994) *Protein Sci. 3*, 2023−2032.
64. Elcock, A., and McCammon, J. A. (1998) *J. Mol. Biol. 280*, 731−748.
65. Yoshida, A. (1964) *Biol. Chem. Hoppe-Seyler 240*, 1118−1124.
66. Madern, D., and Zaccai, G. (1997) *Eur. J. Biochem. 249*, 607−611.
67. Muller, J., Gorisch, H., and Parkhurst, L. J. (1984) *Biochim. Biophys. Acta 787*, 258−263.
68. Steffan, J. S., and McAlister-Henn, L. (1991) *Arch. Biochem. Biophys. 287*, 276−282.
69. Girg, R., Rudolph, R., and Jaenicke, R. (1983) *FEBS Lett. 163*, 132.
70. Jackson, R. M., Gelpi, J. L., Cortes, A., Emery, D. C., Wilks, H., Moreton, K. M., Halsall, D. J., Sleigh, R. N., Behan-Martin, M., Jones, G. R., Clarke, A. R., and Holbrook, J. J. (1992) *Biochemistry 31*, 8307−8314.
71. Cameron, A. D., Roper, D. I., Moreton, K. M., Muirhead, H., Holbrook, J. J., and Wigley, D. B. (1994) *J. Mol. Biol. 238*, 615−625.
72. Abad-Zapatero, C., Griffith, J. P., Sussman, J. L., and Rossmann, M. G. (1987) *J. Mol. Biol. 3*, 445−467.
73. Pappenberger, G., Schuring, H., and Jaenicke, R. (1997) *J. Mol. Biol. 274*, 676−683.

BI9910023